ACS OMEGA

http://pubs.acs.org/journal/acsodf

Article

Tumor-Targeting Ability of Novel Anti-Prostate-Specific Membrane Antigen Antibodies

Hsin-Hua Hsieh, Wei-Ying Kuo, Jia-Jia Lin, Hong-Sen Chen, Hung-Ju Hsu, and Chun-Yi Wu*

Cite This: *ACS Omega* 2022, 7, 31529−31537

Read Online

ACCESS | Metrics & More | Article Recommendations | Supporting Information

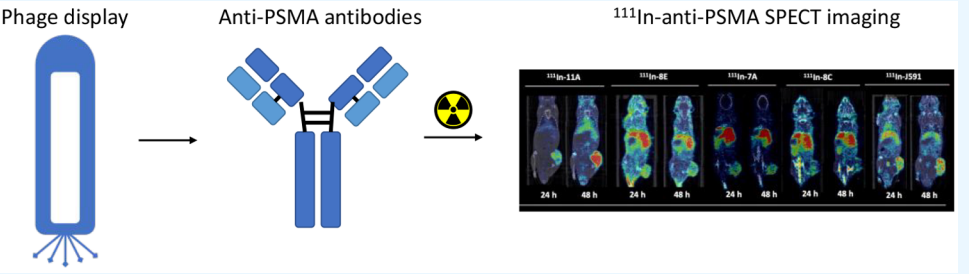

ABSTRACT: Patients with prostate-specific membrane antigen (PSMA)-positive tumors can benefit from PSMA-targeted therapy; thus, we have constructed a phage-displayed synthetic antibody library for the production of novel PSMA antibodies with superior PSMA-targeting ability, favoring clinical management. The binding affinities of anti-PSMA antibodies were verified by an enzyme-linked immunosorbent assay (ELISA). Several in vitro and in vivo experiments, including cellular uptake, internalization, and cytotoxicity studies, micro single photon emission computed tomography (microSPECT)/CT, and biodistribution studies, were performed to select the most promising antibody among six different antibodies. The results showed the target affinities of our antibodies in the ELISA assays (7A, 8C, 8E, and 11A) were comparable to the existing antibodies (J591). The half-maximal effective concentrations of 7A, 8C, 8E, 11A, and J591 were 2.95, 6.64, 5.50, 2.08, and 4.79, respectively. The radiochemical yield of ^{111}In-labeled antibodies ranged from 30% to 50% with high radiochemical purity (>90%). In the cellular uptake studies, the accumulated radioactivity of ^{111}In-J591, ^{111}In-7A, and ^{111}In-11A increased over time. The internalized percentage of ^{111}In-11A was the highest (32.14% ± 2.06%) at 48 h after incubation, whereas that of ^{111}In-J591 peaked at 22.43% ± 4.38% at 24 h and dropped to 13.52% ± 3.03% at 48 h postincubation. Twenty-four hours after injection, radioactivity accumulation appeared in the LNCaP xenografts of the mice injected with ^{111}In-11A, ^{111}In-8E, ^{111}In-7A, and ^{111}In-J591 but not in the xenografts of the ^{111}In-8C-injected group. Marked liver uptake was noticed in all groups except the ^{111}In-11A-injected group. Moreover, the killing effect of ^{177}Lu-11A was superior to that of ^{177}Lu-J591 at low concentrations. In conclusion, we successfully demonstrated that 11A IgG owned the most optimal biological characteristics among several new anti-PSMA antibodies and it can be an excellent PSMA-targeting component for the clinical use.

INTRODUCTION

Prostate cancer (PC) ranked second in cancer incidence and was the fifth-most cause of mortality among men in 2020.[1] Although early stage PC can be curatively treated by surgery or radiation therapy, it is sometimes diagnosed only when metastatic disease has developed. At this stage, the prognosis is poor. Androgen deprivation therapy is the standard treatment for patients with widespread metastases. Unfortunately, almost all metastatic PC will eventually become castration-resistant cancer.

Prostate-specific membrane antigen (PSMA), a type-II transmembrane glycoprotein receptor, is overexpressed on the membrane of most types of PC. Antibody 7E11, first developed by Horoszewicz et al.,[2] targets PSMA-expressing cells, but its clinical application is limited because its binding site locates in an intracellular domain of PSMA.[3] Unlike 7E11, J591 IgG targets the extracellular epitope of PSMA and demonstrates superior binding affinity and rapid clearance from normal organs.[4−6] The J591−PSMA complex also facilitates an antibody-mediated endocytosis process, which has rationalized clinical trials of anti-PSMA antibody-based radiopharmaceutical therapy (RPT). In phase I/II trials, around 8% of patients receiving ^{177}Lu-J591 treatment showed tumor remission and a significant reduction in PSA levels.[7] Although higher doses (70 mCi/m^2) increased the median overall survival of the ^{177}Lu-J591-treated PC patients, they

Received: July 5, 2022
Accepted: August 12, 2022
Published: August 23, 2022

generated more severe side effects such as thrombocytopenia and neutropenia.[8] Recently, a phase I clinical trial demonstrated that alpha-emitted radionuclide ^{225}Ac-labeled J591 mitigates xerostomia and nephrotoxicity in metastatic castration-resistant PC (mCRPC) patients.[9,10] Hammer et al. reported an apparent antitumor activity of ^{227}Th-labeled human anti-PSMA antibody (^{227}Th-PSMA-TTC) against PC in a mouse model.[11] They then launched a clinical trial of the drug for mCRPC patients (NCT03724747).

As intact antibodies have a longer circulation time than small molecules such as PSMA-617, they are cleared more slowly and impose a higher radiation burden on healthy tissues. In imaging, the time interval between the injection and imaging for radiolabeled antibodies must be increased to raise the target-to-background ratio. Although anti-PSMA antibodies are less attractive than small molecules in RPT applications, several clinical trials related to alpha-emitting radionuclide-conjugated antibodies are undergoing. In addition, "active" tumor-targeting nanoparticles[12,13] and antibody−drug conjugates (ADCs)[14,15] still require an antibody with specific tumor-targeting ability and low off-target accumulation in the living body. To fill this need, we prepared some novel anti-PSMA antibodies on the basis of a phage-display library and determined their biological characteristics using a noninvasive imaging method. From the results, we evaluated the clinical potential of the antibodies.

MATERIALS AND METHODS

Preparation of Novel Anti-PSMA Antibodies. The phage-displayed synthetic scFv libraries were constructed and characterized as described in a previous study.[16] The framework sequence of the GH2 scFv library was derived from an J591 antibody sequence and cloned into pCANTAB5E (GE Healthcare) phagemid via *Sfi*I and *Not*I restriction sites. TAA stop codons were introduced in complementarity-determining regions (CDRs) to ensure that only the phagemids carrying the mutagenic oligonucleotides would produce pIII fusion scFv on the phage surface. The framework sequence of the GH2 scFv library was derived from the J591 antibody sequence and cloned into the pCANTAB5E (GE Healthcare) phagemid at the *Sfi*I and *Not*I restriction sites. TAA stop codons were introduced in the CDRs to ensure that only the phagemids carrying the mutagenic oligonucleotides would produce pIII fusion scFv on the phage surface. The positions were mutagenized using synthesized oligonucleotides with the following degenerate codons to produce the designed amino acids in equal molar ratios: Trp/Gly ([T/G]GG), Phe/Ser/Tyr (T[T/C/A][C/T]), Gly/Asp/Ser/Gln ([G/A][G/A][C/T]), Gly/Ala/Ser/Thr/Arg/Pro ([G/A/C][G/C][T/C]), Ala/Thr/Pro/Ser ([A/G/T/C]C[A/G/T/C]), Phe/Tyr/Asp/Val/Asn/Ile/His/Leu ([A/G/T/C][A/T][T/C]), and Leu/Ile/Val/Phe/Met ([A/G/T/C]T[A/G/T/C]). The experimental procedures for the selection and screening of antibodies have been previously published.[12,16−19] To reformat the functional scFvs into the antibodies, the primers, *VLfor* (5′-GGGCCCAGCCGGCCATGGCCGATATTCAAATGACCCAGAGCCCGAGC-3′) with *VLrev* (5′-GGAAGATCTAGAGGAACCACCGCGTTTGATTTCCACTTTGGTGCCTTGACC-3′) and *VHfor* (5′-GGTGGTTCCTCTAGATCTTCCTCCTCTGGTGGCGGTGGCTCGGGCGGTGGTGGGGAAGTGCAGCTGGTGGAATCGGG-3′) with *VHrev* (5′-CCTGCCTGCGGCCGCTGACGCCGAGC-3′) were used in the first PCR. Moreover, in the second PCR, two variable domains were assembled using the overlapping primers: *Overlapfor* (5′-GAGGAGGAGGAGGAGGAGGCGGGGCCCAGCCGGCCATGGCCGATATTC-3′) with *Overlaprev* (5′-GAGGAGGAGGAGGAGGAGCCTGCCTGCGGCCGCTGACGCC-3′). The novel anti-PSMA antibodies were purified on a nickel column and a Superdex 200 increase column for subsequent experiments.

PSMA-Binding Affinity Assays. The binding affinities of anti-PSMA antibodies were determined by an enzyme-linked immunosorbent assay (ELISA). Briefly, the PSMA extracellular domain (ECD) was diluted to 300 ng/mL in phosphate-buffered saline (PBS) and coated on the wells of a 96-well plate (100 μL/well). After 8 h, the solution in each well was replaced by 5% skim milk in PBS with 0.05% Tween 20 (v/v) (PBST) to block the nonspecific binding sites. At 1 h postincubation, anti-PSMA antibodies at various concentrations were added to each well. Each concentration point was performed in triplicate. After a 1 h reaction, the antibody solution was removed and the well was washed thrice with PBST. Horseradish peroxidase-conjugated goat antihuman IgG Fc antibody was added to each well and reacted for another 1 h. After washing with PBST and PBS, 3,3′,5,5′-tetramethylbenzidine was added and reacted for 5 min. Finally, the reaction was stopped by adding 1 N HCl solution. The absorbance was measured at 450 nm.

Preparation of ^{111}In- and ^{177}Lu-Labeled Anti-PSMA Antibodies. The anti-PSMA antibodies modified with diethylenetriaminepentaacetic acid (DTPA) were prepared as previously reported.[20] Briefly, a 5-fold molar excess of DTPA was added to a vial containing anti-PSMA antibodies, and the reaction mixture was kept at 37 °C for 2 h. The crude product was loaded onto a 30 kDa membrane column and centrifuged at 5500*g* for 10 min to remove the unreacted DTPA. This step was repeated twice. For ^{111}In labeling, ^{111}In-$InCl_3$ (37 MBq) and DTPA-conjugated anti-PSMA antibodies (0.1 mg) were added to an Eppendorf tube containing 40 μL of sodium citrate buffer (0.1 M, pH = 5.0). The reaction mixture was allowed to react at 37 °C for 30 min. For ^{177}Lu labeling, ^{177}Lu-$InCl_3$ (18.5 MBq) and DTPA-conjugated anti-PSMA antibodies (0.1 mg) were added to an Eppendorf tube containing 40 μL of sodium citrate buffer (0.1 M, pH = 5.0). The reaction mixture was allowed to react at 37 °C for 50 min. The radiolabeling efficiencies and radiochemical purities of the ^{111}In/^{177}Lu-labeled anti-PSMA antibodies were determined by radio-thin layer chromatography (radioTLC) using an AR2000 scanner (Bioscan, Washington, USA). RadioTLC of the ^{111}In-labeled and ^{177}Lu-labeled antibodies was performed on an instant TLC plate (ITLC, Merck, NewJersy, USA) using sodium citrate buffer (0.5 M, pH = 5.5) as the mobile phase.

Cell Culture and Xenograft Inoculation. The LNCaP human PC cells were cultured in RPMI 1640 medium supplemented with 10% fetal bovine serum (FBS) at 37 °C in a 5% CO_2 atmosphere. The LNCaP cells (1×10^7) in 100 μL of a Matrigel mixture (Matrigel/serum-free medium = 1/1, vol/vol) were inoculated into the right flank of 6-week-old NOD/SCID mice. When the xenograft grew to 100 ± 50 mm^3, the mice were designated to different experiments.

Cellular Uptake and Internalization Assays. Approximately 2×10^6 cells were cultured in a 6-well plate for 1 day. The medium was then replaced by radiolabeled anti-PSMA antibody-containing serum-free medium (~0.22 MBq/well). At 4, 12, 24, and 48 h postincubation, the medium was

https://doi.org/10.1021/acsomega.2c04230
ACS Omega 2022, 7, 31529−31537

aspirated and the well was washed twice with 0.5 mL of iced PBS. The medium and washing buffers were collected into the same counting tube. The coated cells were detached by adding 0.5 mL of 0.25% trypsin, and the well was washed twice with 1 mL of the culture medium. The cell suspension and washing medium were collected into another counting tube. The cellular uptake was expressed as the percentage of administered dose per one million cells (%AD/10^6 cells).

The internalization rates were measured using previously reported methods.[20] Briefly, the cells from the cellular uptake assays were treated with acidic buffer (pH = 2.5) to remove the surface-bound antibodies. The internalization rates were then expressed as a percentage of the radioactivity retained in the cells.

MicroSPECT/CT. MicroSPECT/CT was acquired by the scanner at the Center for Advanced Molecular Imaging and Translation at Chung Gung Memorial Hospital, Taoyuan, Taiwan (nanoSPECT/CT, Mediso, Budapest, Hungary). The xenograft-bearing mice were randomly divided into five groups receiving intravenous injections of different antibodies (^{111}In-11A, ^{111}In-8E, ^{111}In-7A, ^{111}In-8C, or ^{111}In-J591; 18.5 MBq; 0.1 mg IgG/mouse). Static images were acquired at 24 and 48 h postinjection. The tumor-to-muscle (T/M) ratios were calculated from the mean intensities in the regions-of-interest (selected as the tumor and contralateral muscle). The changes in T/M ratios between 24 and 48 h postinjection were calculated as the following relative uptake increments:

$$\text{relative uptake increment (rUI)} = \frac{T/M_{48} - T/M_{24}}{T/M_{24}}$$

where T/M_{24} and T/M_{48} denote the T/M derived from microSPECT at 24 and 48 h postinjection, respectively.

Biodistribution Studies. The mice were intravenously injected with 1.85 MBq of ^{111}In-labeled anti-PSMA antibodies and euthanized at 24 and 48 h postinjection. The tissues and organs, including blood, heart, lung, liver, stomach, small and large intestines, spleen, pancreas, kidney, bone, bone marrow, brain, muscle, and tumor, were excised and weighed. The radioactivity of each tissue/organ was determined by a gamma counter. The uptake was expressed as the percentage of injected dose per gram of tissue (%ID/g).

Cytotoxicity Assays. Approximately 50 000 LNCaP cells were seeded in the wells of a 24-well plate and incubated overnight. Various concentrations of ^{177}Lu-labeled 11A IgG, J591 IgG, or PSMA-617 were added to the culture medium. At 48 h postincubation, the viability of the cells was determined by the 2,5-diphenyl-2*H*-tetrazolium bromide (MTT) assay as previously reported.[21] Briefly, the medium was replaced by the MTT solution (500 μL) and then kept at 37 °C for 3 h. After incubation, the MTT solution was removed and dimethyl sulfoxide solution (1 mL) was added to dissolve the formed crystals. The absorbance at 570 nm was recorded by an ELISA reader (TECAN Trading AG, Mannedorf, Switzerland). The concentration at which the drug killed 50% of the cells (EC_{50}) was calculated from the best-fit curves generated by GraphPad Prism software (version 9.2.0).

Statistical Analysis. All values were expressed as mean ± standard deviation. The Student's t test was applied for the comparison between different groups. Differences with $p < 0.05$ were regarded as statistically different.

RESULTS

Binding Affinity of Anti-PSMA Antibody to Prostate-Specific Membrane Antigen. The antigen-binding affinities of the anti-PSMA antibodies to the PSMA ECD were analyzed by the ELISA assay. The targeting abilities of 7A, 8C, 8E, and 11A were comparable to that of the commercial antibody J591 (Figure 1). The EC_{50} levels of 7A, 8C, 8E, 11A, and J591 were 2.95, 6.64, 5.50, 2.08, and 4.79 ng/mL, respectively.

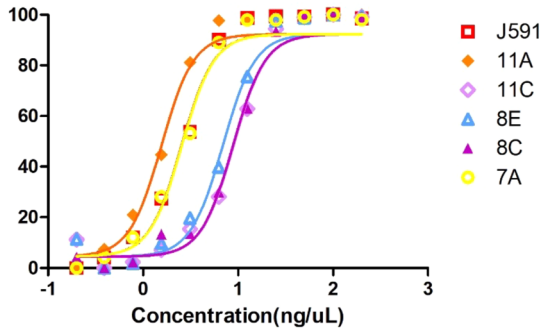

Figure 1. ELISA analysis of anti-PSMA antibodies.

Preparation of ^{111}In-Labeled Antibodies. Figure 2A is a schematic of the ^{111}In-labeling of antibodies. The radiolabeling efficiency of each antibody was around 80%. The uncorrected radiochemical yields of these antibodies ranged from 30% to 50%, and high radiochemical purity (>90%) was observed after purification (Figure 2B).

In Vitro Cellular Uptake and Internalization Assays. The cellular uptakes (expressed as %AD/10^6 cells) of ^{111}In-J591, ^{111}In-7A, and ^{111}In-11A increased over time and were maximized at 25.35 ± 2.36, 4.68 ± 1.00, and 34.26 ± 2.66, respectively, at 48 h postincubation, suggesting that all antibodies specifically targeted PSMA-expressing cells (Figure 3A). The ^{111}In-8E accumulation was significant in the initial stages and plateaued at 24 h after incubation (Figure 3A).

In the internalization assays, ^{111}In-11A alone showed time-dependent behavior and its internalized percentage reached a maximum of 32.14% ± 2.06% at 48 h postincubation, whereas that of ^{111}In-J591 peaked (22.43% ± 4.38%) at 24 h and dropped to 13.52% ± 3.03% at 48 h after incubation (Figure 3B). ^{111}In-8E IgG behaved similarly to ^{111}In-J591, but its maximum internalization level was almost 1.5-fold higher than that of ^{111}In-J591. In contrast, the internalization percentages of 8C and 11D remained low (<5%) throughout the entire experimental period.

MicroSPECT/CT. In each group, apparent liver retention was noticed because macrophages perform robust phagocytosis in the liver. The liver uptake was lowest in the mice injected with ^{111}In-11A (Figure 4). The tumor uptakes, derived from images of ^{111}In-7A, ^{111}In-8C, ^{111}In-8E, ^{111}In-11A, and ^{111}In-J591, were 10.53 ± 2.49, 8.11 ± 3.67, 14.19 ± 1.19, 13.81 ± 2.16, and 20.40% ± 3.12% ID/mL, respectively, at 24 h postinjection and 9.69 ± 3.01, 6.08 ± 3.35, 15.12 ± 2.88, 42.80 ± 3.24, and 25.25% ± 2.35% ID/mL, respectively, at 48 h postinjection. In muscle tissue, the radioactivities of all antibodies except ^{111}In-8C declined over time, as evidenced by their increasing T/M ratios. The relative uptake increments of the ^{111}In-7A-, ^{111}In-8C-, ^{111}In-8E-, ^{111}In-11A-, and ^{111}In-J591-injected mice were 59.0%, −13.6%, 29.2%, 408.1%, and 72.1%, respectively.

https://doi.org/10.1021/acsomega.2c04230
ACS Omega 2022, 7, 31529−31537

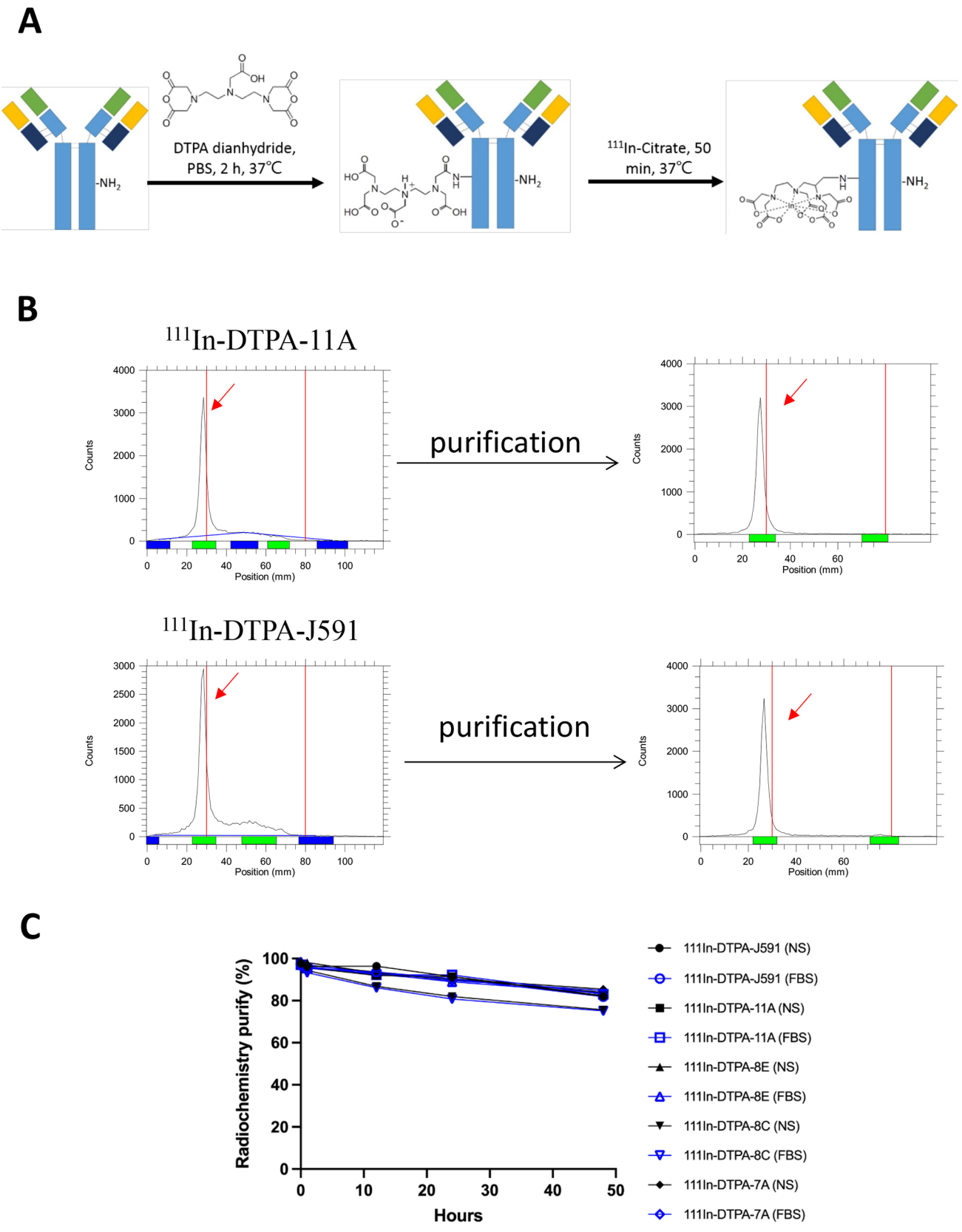

Figure 2. (A) Synthetic scheme of ^{111}In-labeling. (B) RadioTLC of ^{111}In-labeled anti-PSMA antibodies before and after purification. (C) In vitro stability of ^{111}In-labeled anti-PSMA antibodies in either normal saline (NS) or fetal bovine serum (FBS).

Biodistribution Studies. Significant uptakes in the liver, spleen, and kidney were noticed in each group (Figure 5A). The maximum accumulations of ^{111}In-7A, ^{111}In-8E, ^{111}In-11A, and ^{111}In-J591 in the tumor reached 10.53% ± 2.49%, 15.13%

https://doi.org/10.1021/acsomega.2c04230
ACS Omega 2022, 7, 31529−31537

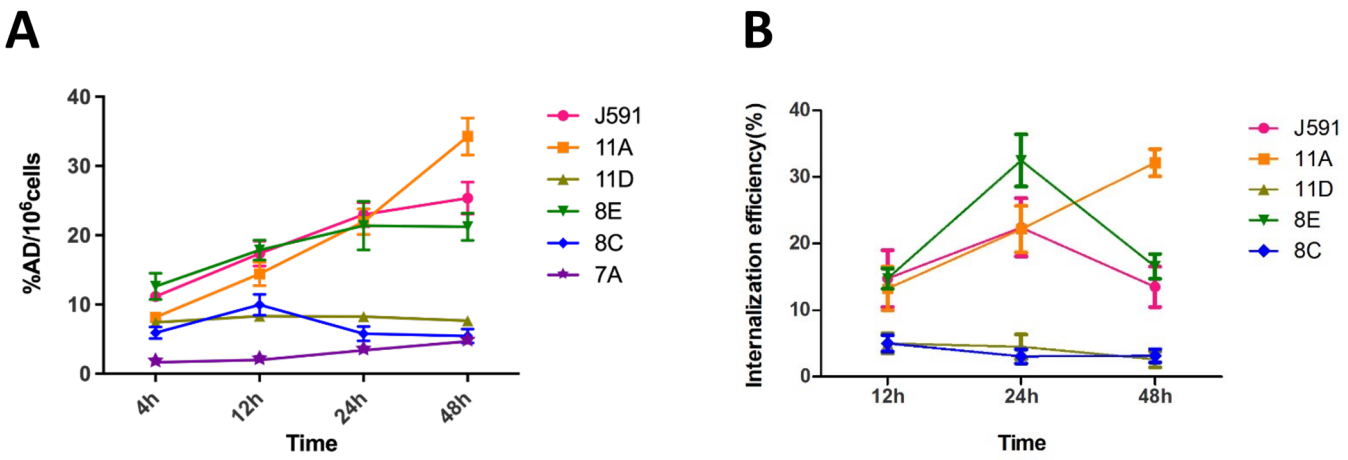

Figure 3. (A) Cellular uptake of ^{111}In-labeled anti-PSMA antibodies in LNCaP human prostate cancer cells at 4, 12, 24, and 48 h postincubation. (B) Internalization of ^{111}In-labeled anti-PSMA antibodies by LNCaP cells with respect to the total amount of cell-bound radioactivity.

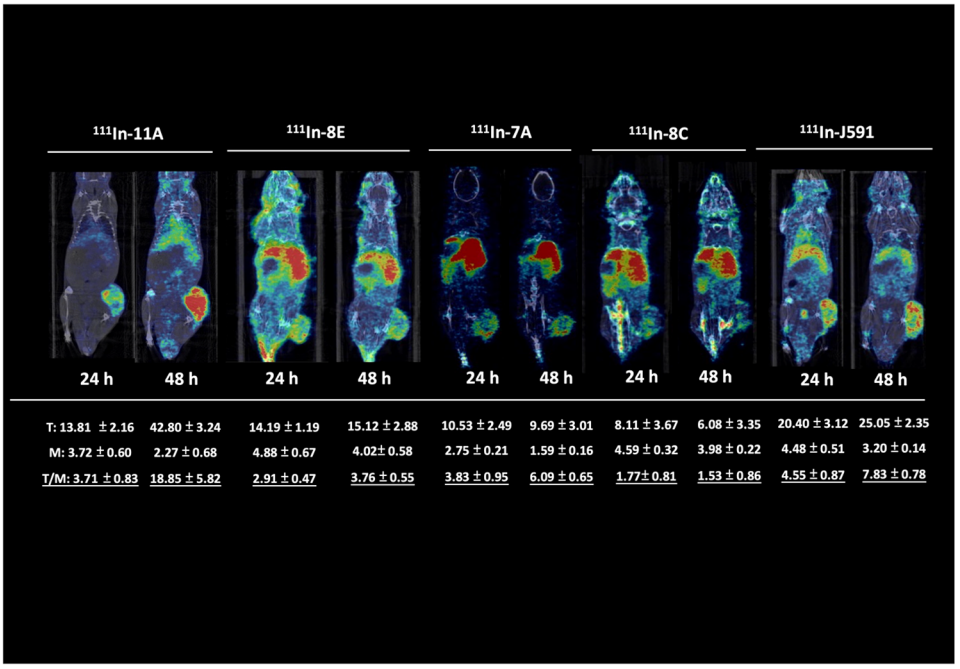

Figure 4. MicroSPECT/CT of LNCaP xenograft-bearing mice injected with 18.5 MBq (0.1 mg IgG/mouse) of ^{111}In-labeled anti-PSMA antibodies at 24 and 48 h postinjection (T = tumor; M = muscle; T/M = tumor-to-muscle ratio).

± 2.88%, 42.80% ± 3.24%, and 25.05% ± 2.35%ID/g, respectively. After 48 h, the T/M ratio of ^{111}In-11A was the highest among the antibodies (Figure 5A). Generally, the results obtained from the biodistrubution studies were in accordance with that derived from the imaging studies. Strong positive correlations were observed between the T/M ratio and rUI acquired from biodistribution and imaging studies at each time points (Figure 5B,C).

Cytotoxicity of ^{177}Lu-Labeled Anti-PSMA Antibodies. The ^{177}Lu-labeling efficiencies of 11A and J591 IgG were around 70% (Figure 6A). After 48 h of incubation, the EC_{50} values of ^{177}Lu-11A, ^{177}Lu-J591, and ^{177}Lu-PSMA-617 were 0.47, 0.82, and 3.84 μCi/mL, respectively. The killing effect of ^{177}Lu-11A was superior to that of ^{177}Lu-J591 at low concentrations, but the effects of both antibodies became similar at higher concentrations (Figure 6C). Unlabeled ^{177}Lu-$LuCl_3$ (free ^{177}Lu) caused no significant cell injury (Figure 6D).

DISCUSSION

PSMA is overexpressed on the membranes of almost all types of PC but is found at limited levels in normal tissues.[22] Considering the low 5-year survival of mCRPC patients, researchers worldwide are committed to developing PSMA-targeting therapeutics. In our previous studies, we synthesized several novel anti-HER2 antibodies with superior targeting capability using a phage-displayed library technique and screened out the antibodies showing minimal off-target retention by a noninvasive imaging method.[20] The potential of the selected antibody, 61 IgG, has also been validated in the development of 61 IgG-modified nanoparticles for boron-neutron capture therapy[12] and anti-HER2 ADCs.[14] In this study, we aimed to duplicate our previous success in the

https://doi.org/10.1021/acsomega.2c04230
ACS Omega 2022, 7, 31529−31537

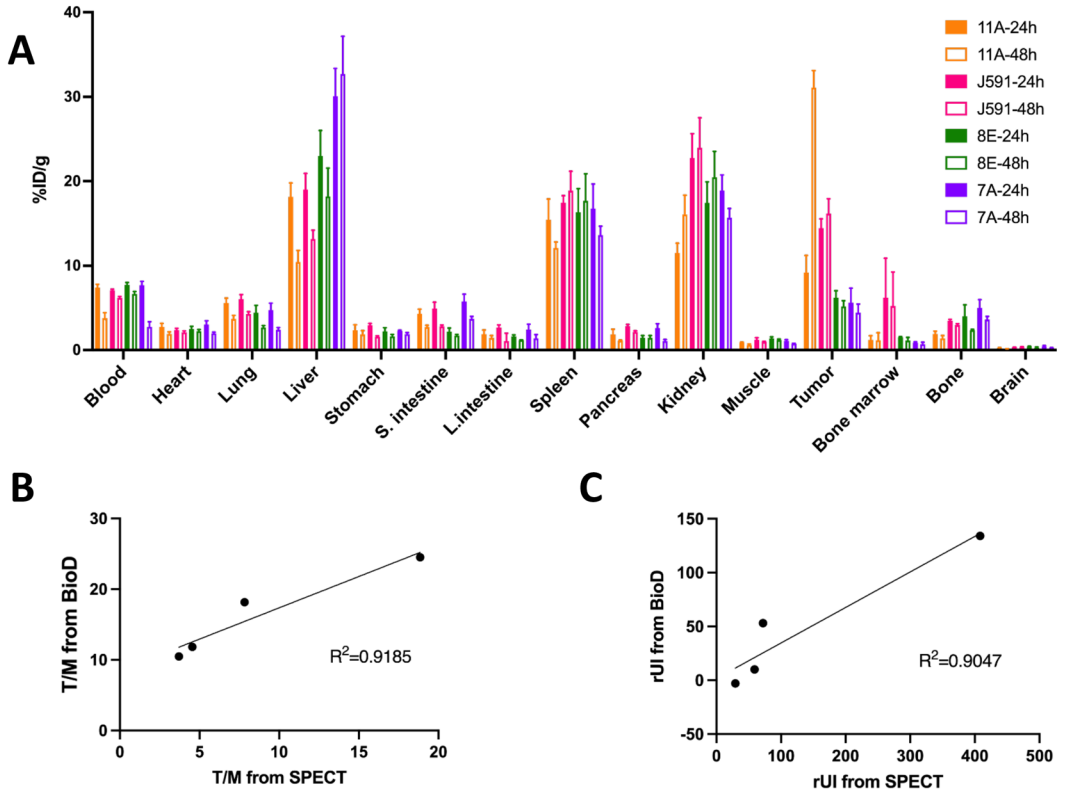

Figure 5. (A) Biodistribution of ^{111}In-labeled antibodies in LNCaP xenograft-bearing mice. (B) Correlation between the tumor-to-muscle ratio (T/M) obtained from biodistribution studies and that derived from SPECT (R^2 = 0.9185, $p < 0.05$). (C) Correlation of relative uptake increment (rUI) obtained from biodistribution studies and that derived from SPECT (R^2 = 0.9047, $p < 0.05$).

identification of anti-PSMA antibodies with optimal biological properties.

J591 IgG is the most commonly used anti-PSMA antibody in modern clinical trials. However, the biological properties of ^{111}In-J591 do not appear to surpass those of ^{111}In-11A IgG. More specifically, the cellular uptake studies showed a time-dependent radioactivity accumulation of ^{111}In-J591, ^{111}In-11A, and ^{111}In-8E IgGs in LNCaP cells, suggesting that these antibodies bind to PC cells over at least 2 days (Figure 3A). Among these antibodies, only 11A IgG showed an increasing internalization rate over time (Figure 3B), which may explain its higher cellular accumulation than the other antibodies (Figure 3A). On the contrary, the nearly unchanged cellular uptake of ^{111}In-8C suggests that it binds to the PSMA but does not induce antibody-mediated endocytosis; accordingly, it stably remains on the cell surface (Figure 3A,B). MicroSPECT confirmed that, in the tumor, the accumulated ^{111}In-11A levels were almost 4-fold higher at 48 h postinjection than at 24 postinjection (Figure 4), implying that antibody-mediated phagocytosis and recycling of PSMAs to the membrane also occurred in vivo. However, the apparent increases in the retained levels of 8E and J591 IgG remained unnoticed because the internalization abilities of these antibodies reduce over time (Figures 3B and 4). α-Particle-emitted radionuclides that conjugate to anti-PSMA antibodies, such as ^{225}Ac-J591 and ^{227}Th-PSMA-TTC (NCT03724747) in clinical trials,[9,10] are restricted because of the limited range of ^{225}Ac, emphasizing the importance of antibody-mediated phagocytosis.

The focus of anti-PSMA RPT has shifted to small-molecule ligands such as ^{177}Lu-PSMA-617 and ^{177}Lu-PSMA I&T[23] because the large molecular weight of antibodies elevates the required time for clearance and potentially increases the radiation burden to normal tissues. ^{89}Zr-J591 imaging confirmed that antibodies are intensely uptaken by the liver and are cleared slowly from the living body.[24] The injection-to-scan acquisition time interval of ^{89}Zr-J591 imaging with a satisfactory tumor-to-background ratio was 8 days.[24] However, monoclonal antibodies generally have low off-target toxicity in the body because they specifically attach to the target. Moreover, unlike ^{177}Lu-PSMA-617, J591 IgG is not retained in the salivary and lacrimal glands so cannot cause severe xerostomia.[24] The primary dose-limiting side effect of ^{177}Lu-J591 is myelosuppression.[8] In the present study, ^{111}In-11A (unlike ^{111}In-J591) was minimally uptaken by the salivary glands and kidneys (Figure 4). In addition, we observed that 11A IgG accumulated to significantly lower levels than J591 in bone marrow (Figure 5A); therefore, it might mitigate the severity of myelosuppression.

On the basis of previous studies, the use of DOTA in radiolabeling needs an elevated temperature (sometimes close to 100 °C), which would greatly affect the reactivity of the antibodies.[25−27] Second, the metal impurities, such as Ca^{2+}, Zn^{2+}, and Fe^{2+}, produced in the production of Lu-177, are competitors for DOTA chelation in the labeling, possibly resulting in an unsatisfactory radiochemical yield. However, Brom et al. and Watanabe et al. indicated that these impurities affect the labeling efficiency of DTPA-modified antibodies to a lesser extent.[25,28] Besides, the thermodynamic stability constant (Log_{KML}) of the [^{177}Lu(III)-DTPA] complex is nearly identical with that of [^{177}Lu(III)-DOTA],[29] suggesting the stability of ^{177}Lu-DTPA-11A may not be the issue. Our

https://doi.org/10.1021/acsomega.2c04230
ACS Omega 2022, 7, 31529−31537

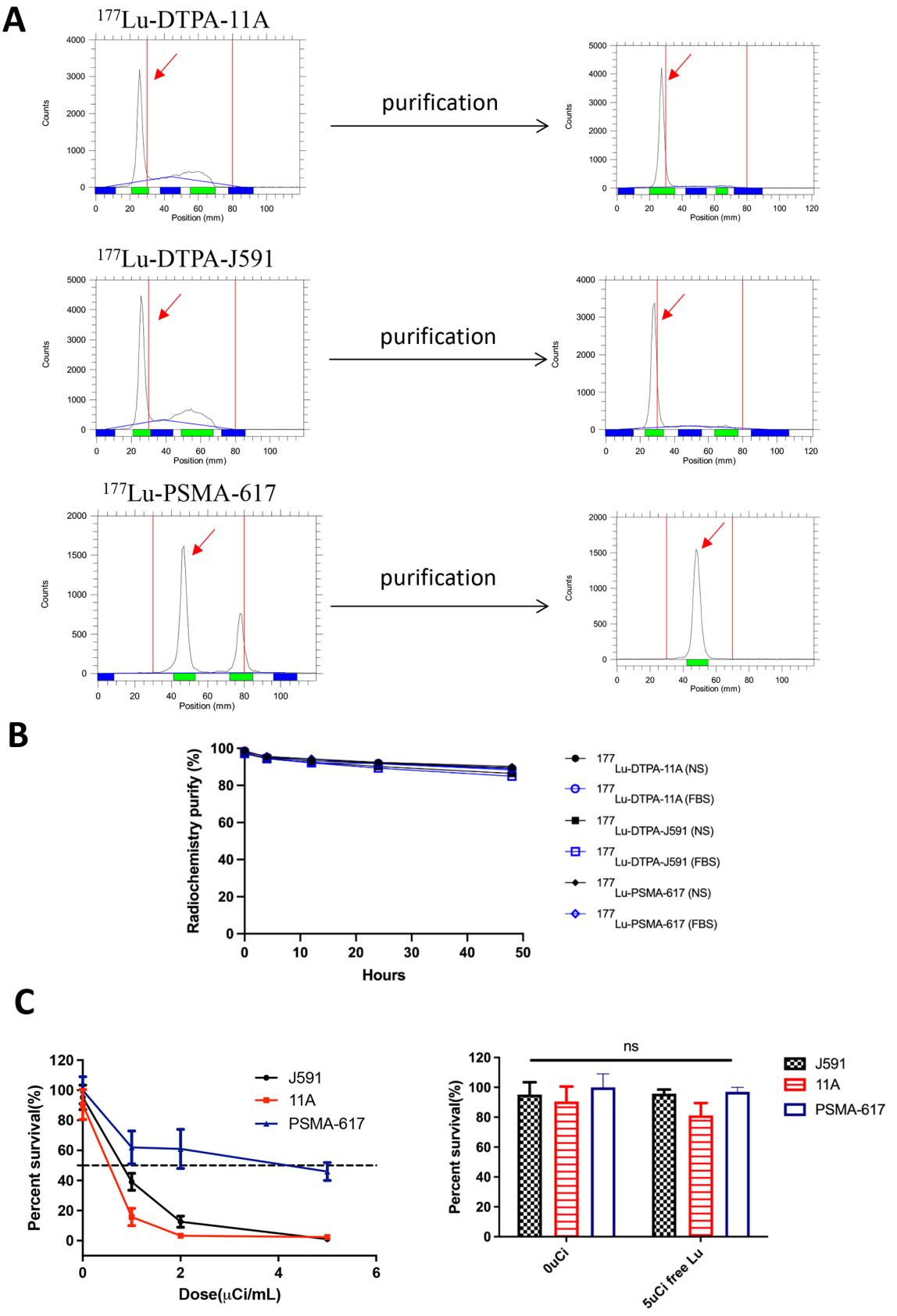

Figure 6. (A) RadioTLC of ^{177}Lu-labeled 11A IgG, J591 IgG, and PSMA-617 before and after purification. (B) In vitro stability of ^{177}Lu-labeled 11A IgG, J591 IgG, and PSMA-617 in either normal saline (NS) or fetal bovine serum (FBS). (C) In vitro killing effect of ^{177}Lu-labeled 11A IgG, J591 IgG, and PSMA-617.

https://doi.org/10.1021/acsomega.2c04230
ACS Omega 2022, 7, 31529−31537

results also confirmed the stability of ^{177}Lu-DTPA-11A is quite high during the entire experimental period (Figure 6B). According to these points, we selected DTPA as the chelate in this proof-of-concept study. ^{177}Lu-11A (~45%) achieved a slightly lower radiochemical yield than ^{177}Lu-J591 (~45% vs ~60%) but was more stable than ^{177}Lu-J591 (Figure 6B). ^{177}Lu-11A exerted a more evident in vitro antitumoral effect than ^{177}Lu-J591 and even ^{177}Lu-PSMA-617 (Figure 6C). The present study was limited to evaluating the PSMA-targeting ability of our self-synthesized antibodies; we did not investigate the in vivo characteristics of ^{177}Lu-11A. As the US Food and Drug Administration has approved ^{177}Lu-PSMA-617 for patients with PSMA-positive mCRPC, there is an increasing need for immunohistochemistry (IHC) staining of tumors with high PSMA affinity and specificity. On the basis of our results, 11A IgG could also serve as a reliable primary antibody against PSMA for IHC staining.

CONCLUSION

We successfully developed and tested several novel anti-PSMA antibodies. The in vitro and in vivo tumor-targeting abilities of 11A IgG were comparable to or superior to those of commercial J591 IgG. The current data demonstrated the excellent potential of 11A IgG as a targeting component for conjugation with therapeutic radionuclides, drugs, or modified membranes of nanoparticles.

ASSOCIATED CONTENT

Supporting Information

The Supporting Information is available free of charge at https://pubs.acs.org/doi/10.1021/acsomega.2c04230.

Results of ELISA and radiolabeling of each anti-PSMA antibody (PDF)

AUTHOR INFORMATION

Corresponding Author

Chun-Yi Wu − *Department of Biomedical Imaging and Radiological Sciences, National Yang Ming Chiao Tung University, Taipei 112, Taiwan;* orcid.org/0000-0002-8217-1692; Email: chunyiwu@nycu.edu.tw

Authors

Hsin-Hua Hsieh − *Department of Biomedical Imaging and Radiological Sciences, National Yang Ming Chiao Tung University, Taipei 112, Taiwan*

Wei-Ying Kuo − *Genomics Research Center, Academia Sinica, Taipei 115, Taiwan*

Jia-Jia Lin − *Department of Nuclear Medicine, New Taipei Municipal TuCheng Hospital (Built and Operated by Chang Gung Medical Foundation), New Taipei City 236, Taiwan*

Hong-Sen Chen − *Genomics Research Center, Academia Sinica, Taipei 115, Taiwan*

Hung-Ju Hsu − *Genomics Research Center, Academia Sinica, Taipei 115, Taiwan*

Complete contact information is available at: https://pubs.acs.org/10.1021/acsomega.2c04230

Funding

This research was funded by the Ministry of Science and Technology of Taiwan (MOST 108-2314-B-010-062) and Atomic Energy Council of Taiwan (MOST 111-2623-E-A49-004-NU).

Notes

The authors declare no competing financial interest.

ACKNOWLEDGMENTS

All animal studies were approved by the Institutional Animal Care and Use Committee of the China Medical University (CMUIACUC-2019-104) and National Yang Ming Chaio Tung University (IACUC No. 1100318). We are thankful for the technical support from the Laboratory Animal Center of LinKou Chang Gung Memorial Hospital and Instrumentation Resource Center of National Yang Ming Chiao Tung University.

REFERENCES

(1) Sung, H.; Ferlay, J.; Siegel, R. L.; Laversanne, M.; Soerjomataram, I.; Jemal, A.; Bray, F. Global cancer statistics 2020: GLOBOCAN estimates of incidence and mortality worldwide for 36 cancers in 185 countries. *Ca-Cancer J. Clin.* **2021**, *71*, 209−49.

(2) Horoszewicz, J. S.; Kawinski, E.; Murphy, G. P. Monoclonal antibodies to a new antigenic marker in epithelial prostatic cells and serum of prostatic cancer patients. *Anticancer Res.* **1987**, *7*, 927−935.

(3) Akhtar, N. H.; Pail, O.; Saran, A.; Tyrell, L.; Tagawa, S. T. Prostate-specific membrane antigen-based therapeutics. *Adv. Urol.* **2012**, *2012*, 973820.

(4) Liu, H.; Moy, P.; Kim, S.; Xia, Y.; Rajasekaran, A.; Navarro, V.; Knudsen, B.; Bander, N. H. Monoclonal antibodies to the extracellular domain of prostate-specific membrane antigen also react with tumor vascular endothelium. *Cancer Res.* **1997**, *57*, 3629−3634.

(5) Smith-Jones, P. M.; Vallabahajosula, S.; Goldsmith, S. J.; Navarro, V.; Hunter, C. J.; Bastidas, D.; Bander, N. H. In vitro characterization of radiolabeled monoclonal antibodies specific for the extracellular domain of prostate-specific membrane antigen. *Cancer Res.* **2000**, *60*, 5237−5243.

(6) Smith-Jones, P. M.; Vallabhajosula, S.; Navarro, V.; Bastidas, D.; Goldsmith, S. J.; Bander, N. H. Radiolabeled monoclonal antibodies specific to the extracellular domain of prostate-specific membrane antigen: preclinical studies in nude mice bearing LNCaP human prostate tumor. *J. Nucl. Med.* **2003**, *44*, 610−617.

(7) Bander, N. H.; Milowsky, M. I.; Nanus, D. M.; Kostakoglu, L.; Vallabhajosula, S.; Goldsmith, S. J. Phase I trial of 177lutetium-labeled J591, a monoclonal antibody to prostate-specific membrane antigen, in patients with androgen-independent prostate cancer. *J. Clin Oncol.* **2005**, *23*, 4591−601.

(8) Tagawa, S. T.; Milowsky, M. I.; Morris, M.; Vallabhajosula, S.; Christos, P.; Akhtar, N. H.; Osborne, J.; Goldsmith, S. J.; Larson, S.; Taskar, N. P.; et al. Phase II study of Lutetium-177-labeled anti-prostate-specific membrane antigen monoclonal antibody J591 for metastatic castration-resistant prostate cancer. *Clin. Cancer Res.* **2013**, *19*, 5182−91.

(9) Tagawa, S. T.; Osborne, J.; Niaz, M. J.; Vallabahajosula, S.; Vlachostergios, P. J.; Thomas, C.; Molina, A. M.; Sternberg, C. N.; Singh, S.; Fernandez, E.; et al. Dose-escalation results of a phase I study of 225Ac-J591 for progressive metastatic castration resistant prostate cancer (mCRPC). *J. Clin Oncol.* **2020**, *38*, 114.

(10) Tagawa, S. T.; Sun, M.; Sartor, A. O.; Thomas, C.; Singh, S.; Bissassar, M.; Fernandez, E.; Niaz, M. J.; Ho, B.; Vallabahajosula, S.; et al. Phase I study of 225Ac-J591 for men with metastatic castration-resistant prostate cancer (mCRPC). *J. Clin Oncol.* **2021**, *39*, 5015.

(11) Hammer, S.; Hagemann, U. B.; Zitzmann-Kolbe, S.; Larsen, A.; Ellingsen, C.; Geraudie, S.; Grant, D.; Indrevoll, B.; Smeets, R.; von Ahsen, O.; et al. Preclinical Efficacy of a PSMA-Targeted Thorium-227 Conjugate (PSMA-TTC), a Targeted Alpha Therapy for Prostate Cancer. *Clin. Cancer Res.* **2020**, *26*, 1985−96.

(12) Wu, C. Y.; Lin, J. J.; Chang, W. Y.; Hsieh, C. Y.; Wu, C. C.; Chen, H. S.; Hsu, H. J.; Yang, A. S.; Hsu, M. H.; Kuo, W. Y. Development of theranostic active-targeting boron-containing gold

nanoparticles for boron neutron capture therapy (BNCT). *Colloids Surf. B Biointerfaces.* **2019**, *183*, 110387.
(13) Fay, F.; Scott, C. J. Antibody-targeted nanoparticles for cancer therapy. *Immunotherapy.* **2011**, *3*, 381−94.
(14) Kuo, W. Y.; Hsu, H. J.; Wu, C. Y.; Chen, H. S.; Chou, Y. C.; Tsou, Y. L.; Peng, H. P.; Jian, J. W.; Yu, C. M.; Chiu, Y. K.; et al. Antibody-drug conjugates with HER2-targeting antibodies from synthetic antibody libraries are highly potent against HER2-positive human gastric tumor in xenograft models. *MAbs.* **2019**, *11*, 153−65.
(15) Diamantis, N.; Banerji, U. Antibody-drug conjugates–an emerging class of cancer treatment. *Br J. Cancer.* **2016**, *114*, 362−7.
(16) Chen, H. S.; Hou, S. C.; Jian, J. W.; Goh, K. S.; Shen, S. T.; Lee, Y. C.; You, J. J.; Peng, H. P.; Kuo, W. C.; Chen, S. T.; et al. Predominant structural configuration of natural antibody repertoires enables potent antibody responses against protein antigens. *Sci. Rep.* **2015**, *5*, 12411.
(17) Hou, S. C.; Chen, H. S.; Lin, H. W.; Chao, W. T.; Chen, Y. S.; Fu, C. Y.; Yu, C. M.; Huang, K. F.; Wang, A. H.; Yang, A. S. High throughput cytotoxicity screening of anti-HER2 immunotoxins conjugated with antibody fragments from phage-displayed synthetic antibody libraries. *Sci. Rep.* **2016**, *6*, 31878.
(18) Tung, C. P.; Chen, I. C.; Yu, C. M.; Peng, H. P.; Jian, J. W.; Ma, S. H.; Lee, Y. C.; Jan, J. T.; Yang, A. S. Discovering neutralizing antibodies targeting the stem epitope of H1N1 influenza hemagglutinin with synthetic phage-displayed antibody libraries. *Sci. Rep.* **2015**, *5*, 15053.
(19) Hsu, H. J.; Lee, K. H.; Jian, J. W.; Chang, H. J.; Yu, C. M.; Lee, Y. C.; Chen, I. C.; Peng, H. P.; Wu, C. Y.; Huang, Y. F.; et al. Antibody variable domain interface and framework sequence requirements for stability and function by high-throughput experiments. *Structure.* **2014**, *22*, 22−34.
(20) Kuo, W. Y.; Lin, J. J.; Hsu, H. J.; Chen, H. S.; Yang, A. S.; Wu, C. Y. Noninvasive assessment of characteristics of novel anti-HER2 antibodies by molecular imaging in a human gastric cancer xenograft-bearing mouse model. *Sci. Rep.* **2018**, *8*, 13735.
(21) Wu, C. Y.; Tang, J. H.; Chan, P. C.; Li, J. J.; Lin, M. H.; Shen, C. C.; Liu, R. S.; Wang, H. E. Monitoring Tumor Response after Liposomal Doxorubicin in Combination with Liposomal Vinorelbine Treatment Using 3′-Deoxy-3′-[(18)F]Fluorothymidine PET. *Mol. Imaging Biol.* **2017**, *19*, 408−20.
(22) Ghosh, A.; Heston, W. D. Tumor target prostate specific membrane antigen (PSMA) and its regulation in prostate cancer. *J. Cell Biochem.* **2004**, *91*, 528−39.
(23) Jones, W.; Griffiths, K.; Barata, P. C.; Paller, C. J. PSMA Theranostics: Review of the Current Status of PSMA-Targeted Imaging and Radioligand Therapy. *Cancers (Basel).* **2020**, *12*, 1367.
(24) Pandit-Taskar, N.; O'Donoghue, J. A.; Durack, J. C.; Lyashchenko, S. K.; Cheal, S. M.; Beylergil, V.; Lefkowitz, R. A.; Carrasquillo, J. A.; Martinez, D. F.; Fung, A. M.; et al. A Phase I/II Study for Analytic Validation of 89Zr-J591 ImmunoPET as a Molecular Imaging Agent for Metastatic Prostate Cancer. *Clin. Cancer Res.* **2015**, *21*, 5277−85.
(25) Brom, M.; Joosten, L.; Oyen, W. J. G.; Gotthardt, M.; Boerman, O. C. Improved labelling of DTPA- and DOTA-conjugated peptides and antibodies with 111In in HEPES and MES buffer. *EJNMMI Research.* **2012**, *2*, 4.
(26) Liu, F.; Zhu, H.; Yu, J.; Han, X.; Xie, Q.; Liu, T.; Xia, C.; Li, N.; Yang, Z. (68)Ga/(177)Lu-labeled DOTA-TATE shows similar imaging and biodistribution in neuroendocrine tumor model. *Tumour Biol.* **2017**, *39*, 101042831770551.
(27) Rizvi, S. F. A.; Naqvi, S. A. R.; Roohi, S.; Sherazi, T. A.; Rasheed, R. (177)Lu-DOTA-coupled minigastrin peptides: promising theranostic agents in neuroendocrine cancers. *Mol. Biol. Rep.* **2018**, *45*, 1759−67.
(28) Watanabe, S.; Hashimoto, K.; Ishioka, N. S. Lutetium-177 complexation of DOTA and DTPA in the presence of competing metals. *J. Radioanal. Nucl. Chem.* **2015**, *303*, 1519−1521.
(29) Spreckelmeyer, S.; Ramogida, C. F.; Rousseau, J.; Arane, K.; Bratanovic, I.; Colpo, N.; Jermilova, U.; Dias, G. M.; Dude, I.; Jaraquemada-Peláez, M. d. G.; et al. p-NO2−Bn−H4neunpa and H4neunpa−Trastuzumab: Bifunctional Chelator for Radiometalpharmaceuticals and 111In Immuno-Single Photon Emission Computed Tomography Imaging. *Bioconjugate Chemistry.* **2017**, *28*, 2145−2159.

https://doi.org/10.1021/acsomega.2c04230
ACS Omega 2022, 7, 31529−31537